



"Gheorghe Asachi" Technical University of Iasi, Romania



EXPERIMENTAL INVESTIGATION OF FORCED EVAPORATION COEFFICIENT FROM THE DISTURBED SURFACE OF HEATED WATER

Dariusz Obracaj*, Marek Korzec, Klaudia Zwolińska

AGH University of Science and Technology, Department of Environmental Engineering
Mickiewicz Av. 30, 30-059 Krakow, Poland

Abstract

This article presents the results of laboratory tests of water evaporation for varying air velocities over the water surface at different water wave heights. Measurements of water evaporation were conducted using the experimental setup, which consists of a wind tunnel covering a bottom-heated water tank. The investigations were carried out for water temperature higher than the intake air temperature in the range of variable air velocity from 0.40 to 0.94 m/s. The measurements were carried out for four series with heights of spatter-free wave 0, 1.5, 3.0 and 5.0 mm, respectively. The conditions were maintained in such a way that the variations in the partial pressure over the water surface were kept to a minimum. The evaporation coefficient was defined, as the water mass transfer coefficient referred to the steady differential of water vapour partial pressures at air and water temperatures. The novelty consists in finding a linear correlation between the evaporation coefficient and the air velocity over the disturbed water surface. However, an increase in the evaporation coefficient is directly proportional to the height of the water wave. By comparing the wave height to the coefficient of pool occupancy, a new formula for predicting evaporation is given for indoor pools.

Key words: evaporation coefficient, humidity, temperature, thermal pool, water evaporation rate

Received: January, 2020; *Revised final:* July, 2020; *Accepted:* October, 2020; *Published in final edited form:* February, 2021

1. Introduction

The main task of ventilation systems in indoor pools, apart from providing outdoor air, is to ensure comfort conditions to its occupants. Proper calculations of moisture gains and losses allow for designing air-conditioning, as well as estimating energy demand for a building (Shah, 2013) or saving water consumption, which can be determined by the water footprint indicator (Matarazzo, 2017). In indoor pools with increased moisture gains, it is therefore essential to estimate the moisture flow to the indoor air as precisely as possible, which implicates selecting and operating an air-conditioning system.

The water evaporation phenomenon is dependent on the physical and thermodynamic

parameters of water and air. Additionally, it also depends on the extent of the disturbance of the water surface associated with a number of people and their activity (Smith et al., 1998; Shah, 2012, 2018). For engineering applications, the prediction of the water evaporation rate is essential to the design of low-energy air-conditioning systems for such buildings.

Investigation results of the influence of water and air temperatures as well as air velocity over a free (undisturbed) water surface are most accurate. The impact of these factors on the evaporation phenomenon has been known since John Dalton conducted a theoretical discussion on the phenomenon of water evaporation in 1802. Then, many investigators specified the effect of water and air factors in the drive of the intensity of mass and energy

* Author to whom all correspondence should be addressed: e-mail: obracaj@agh.edu.pl; Phone: +48 12 6172180

exchange between them. In an historical approach, the most-known works belong to: Carrier (1918), Himus and Hinchley (1924), Powell and Griffiths (1935), Lurie and Michailoff (1936), Meyer (1942), Malicki (1962), Baturin (1972), Biasin and Krumme (1974). Many investigations have been carried out in the last two decades. These works include, above all: Asdrubali et al. (2009), Blázquez et al. (2017), Hens (2009), Hugo (2015), Poós and Varjul (2019), Raimundo et al., (2014), Smith et al. (1993, 1994, 1998), Sartori (2000), Shah (2003, 2008, 2012, 2013, 2014, 2018), and many others. Many of these works present empirical correlations based on laboratory experiments using laboratory tanks and vessels containing water, containers with wind tunnels or evaporation pans. The comparisons of various analytical and empirical correlations in the prediction of water evaporation were presented by both Sartori (2000) and Poós and Varjul (2019).

Some of the authors see an effective method in CFD modelling due to the difficulties in investigating full-scale water pools. Blázquez et al. (2017) in their research, compared the results obtained in the measurements to that defined in the CFD program, ANSYS Fluent 17.1. The authors carried out investigations both on scale models and on an original swimming-pool, and then performed calculations using CFD methods, assuming different convection processes. They achieved compatibility of research results and numerical modelling, with an average relative error of 3.3% for the original swimming-pool. Finally, they referred the dependence of the error in the estimated evaporation rate on the different convection mechanism to the dimensionless product Gr_m / Re_L^2 , which approximates the buoyancy and inertial forces (Blázquez et al., 2017).

Similarly, Ciuman and Lipska (2018) compared the validated CFD model with known analytical methods of the calculation of the evaporation rate. They accepted the results of the measurements carried out on an original object as boundary conditions needed for numerical calculations. The analysis carried out by the researchers shows that the results obtained from CFD model are the closest to the German VDI standard method (VDI 2089, 2010). The method can also be found for estimating the evaporation rate based on neural networks in a large body of literature. Lu et al. (2014) proposed a new evaporation model from pool surfaces, treating evaporation as a dynamic process, in which the superiority of this method is perceived.

The process of water evaporation may take place under the influence of natural, forced or transition convection processes, respectively. The natural convection-driven evaporation process is well recognised, which is indicated, among other things, in works by Asdrubali et al. (2009), Bower and Saylor (2009), Kumar and Arakeri (2015), Poós and Varjul (2019), Sartori (2000). The investigations of the forced convection influence focused more on outdoor swimming pools (Smith et al., 1994; Tang and Etzion, 2004). As mentioned before, according to Dalton, the

water mass transfer is dependent on the partial pressure difference. Almost all the general evaporation rate form given by Dalton may be formulated as given by Eq. (1):

$$E = \frac{h_e \cdot (p_w - p_a)}{h_w} \quad (1)$$

In the case of a natural effect without forced convection mechanisms, nonlinear changes in the evaporation rate were found depending on the difference in partial pressures. Most often, in this case, it is given by the exponential function of the pressure difference, as demonstrated by numerous investigators: Himus and Hinchley (1924); Pauken (1999), Tang and Etzion (2004), or it depends on both vapour pressure difference and vapour density difference, as indicated by Jodat et al. (2012). However, as it has been proven (Blázquez et al., 2017; Pauken, 1999;) that water evaporation in indoor pools may occur under laminar and turbulent conditions for both the free and forced convection mechanisms. This effect was described by Pauken (1999) as a mixed massive convective effect.

The linear relationship between the evaporation rate and the difference of air-water partial pressure, both for turbulent and transition regimes, has already been confirmed, among others, by Pauken (1999) and Sartori (2000). Therefore, the mass flow rate of evaporated water can be predicted by Eq. (2):

$$m_{H_2O} = \frac{h_e \cdot (p_w - p_a)}{h_w} \cdot A_{ws} \quad (2)$$

Sometimes the evaporation water rate refers not to the pressure difference (Pauken, 1999), especially when exposed to free convection, but the difference of densities at the water-air interface. In turn, if the assumption of a unit differential of water vapour partial pressures is accepted, then the equation in (Eq. 1) may be presented using evaporation coefficient ε given by (Eq. 3):

$$E = \varepsilon \cdot (p_{ws} - p_w) \quad (3)$$

Evaporation coefficient ε is not usually shown in many evaporation rate formulas, but it is often replaced by a function of the velocity of air moving over the water surface, $\varepsilon = a \cdot v_{ws} + b$. Coefficients a and b of this linear relationship are constant under the water-air interface conditions (Sartori, 2000; Shah, 2013). Various authors provide the values of these coefficients. The nature of an object, a type of an indoor pool and the size of water surface disturbance are taken into account when determining the most appropriate values. The most popular coefficients include the evaporation coefficients according to such authors as Biasin and Krumme (1974), Carrier (1918), Hens (2009), Smith et al. (1998), Shah (2003, 2008),

A wide range of correlations is available in the body of literature for predicting water evaporation

rates on free water surfaces. However, investigations on evaporation from a disturbed water surface have rarely been undertaken, probably due to the lack of vision about their practical usefulness. Most often, they refer to a type of a pool or a factor representing a number of people using the pool. The most commonly used empirical correlations related to the prediction of evaporation from disturbed water surfaces or indoor pool types are given in Table 1. The ASHRAE Handbook (2015) recommends the use of Carrier's correlation. The empirical equation is given in Table 1. Eq. (4) may be modified by multiplying it by activity factor F_a to estimate the evaporation rate based on the level of activity supported (Table 1).

The data from the German industry standard VDI, which takes a type of an indoor pool into consideration, are also often used in Europe. Each of them can be used in other solutions because they take into account different criteria. The disturbance of the water surface was often related to a number of people inside the water pool, as indicated by German researchers in the 20th century. First Biasin and Krume (1974) and later Smith et al. (1994) and in turn Shah (2003) proved that an increase in evaporation associated with the occupancy concerning evaporation from free water surface E_0 could be a factor showing the impact of users on the water evaporation in indoor pools.

According to Smith et al. (1998) the evaporation rate for occupied pools is characterized by evaporation ratio E_R , which compares the evaporation rate during the occupancy of a pool to the evaporation from an inactive pool in the same conditions. The authors presented evaporation ratio E_R as a function of a number of people per surface and they proposed

the relation (Eq. 7) presented in Table 1. They have specified that the disturbance and motion of the water surface caused by typical swimming activity increases evaporation rates to levels of approximately 70% higher than those from free water surfaces in indoor pools.

Shah (2013), presents a method for determining the evaporation rate for occupied swimming pools. However, research shows that indoor pools during occupation are characterized by higher water evaporation due to an increased contact area between water and air, through water rippling, wet floors and occupants' wet bodies. Shah also drew attention to the significant impact of the difference in air density in the room and the contact area with the water surface.

Therefore, the formula proposed by the author takes into account both the difference in air density and a number of users of the facility. In his publication (Shah, 2014), the author refers to the standard International Building Code 2006, in which for indoor swimming pools, maximum one person per 4.5 m² of the water surface is assumed. The author presents the dependence of evaporation growth based on the correction factor depending on pool utilization factor $F_U = 4.5 \cdot N^*$. According to work (Shah, 2018), the author presents three formulas describing an increase in the evaporation rate depending on utilization factor U . Shah (2018) considers value $U > 1$ to be too high due to a large number of occupants and assumes that an increase in evaporation is permanent. For such a condition, he assumes that an increase in the evaporation coefficient is 2.5 times. In this publication (Shah, 2018), he improves the empirical correlation of water evaporation for unoccupied pools.

Table 1. Various correlations for the prediction of evaporation coefficient ε from disturbed water surface in indoor pools

Author	Formula*	No.	Notes	Unofficial description	Typical activity factor	Type of Pool
ASHRAE (2015)	$\varepsilon = 3.6 \cdot \frac{0.089 + 0.0782 \cdot v_{ws}}{h_w} \cdot F_a$	(4)	Evaporation coefficient calculated according to the Carrier's formula for active pools. The formula recommended for h_w values of about 2400 kJ/kg and air velocities values ranging from 0.05 to 0.15 m/s. Activity factor F_a is determined based on a type of object. It is recommended to simplify $\varepsilon = 4 \cdot 10^{-5} \cdot F_a$ for indoor pools.	ASHRAE-0	$F_a = 0.5$	Baseline (pool unoccupied)
				ASHRAE-1	$F_a = 0.5$	Residential pools
				ASHRAE-2	$F_a = 0.65$	Condominium pools
				ASHRAE-3	$F_a = 0.65$	Therapy pools
				ASHRAE-4	$F_a = 0.8$	Hotel
				ASHRAE-5	$F_a = 1.0$	Public, schools
				ASHRAE-6	$F_a = 1.0$	Whirlpools, spas
			ASHRAE-7	$F_a = 1.5$ (minimum)	Wavepools, water slides	
VDI 2089 (2010)	$\varepsilon = 1 \cdot 10^{-5} \cdot \beta$	(5)	Selection depending on the functionality of an	VDI-1	$\beta = 15$	for private swimming pool, not very

			object. It is recommended $\beta = 5$ for free surface of water.		occupied for public swimming pool, (normal activity)
				VDI-2	$\beta = 20$
				VDI-3	$\beta = 28$
				VDI-4	$\beta = 35$
					for wave pool
Smith et al. (1998)	$\varepsilon = 0.0000106 \cdot E_R$ $E_R = \frac{E}{E_0} = \frac{\varepsilon}{\varepsilon_0} = 1.04 + 4.27 \cdot N^*$ $\varepsilon_0 = 3.6 \cdot \frac{0.06428 + 0.06235 \cdot v_{ws}}{h_w}$	(6) (7) (8)	Dependence based on tests carried out in a public indoor pool. Evaporation coefficient for a free surface is determined according to formula (Eq. 8).		
Shah (2003) empirical	$E = 0.113 - \frac{0.000079}{F_u} + 0.000059 \cdot (p_{ws} - p_a)$ $\varepsilon = \frac{E}{(p_{ws} - p_a)}$	(9) (9a)	F_u is a pool utilization factor, $F_u = 4.5 \cdot N^*$. This equation was based on data for $F_u > 0.1$. For $F_u > 1$, we use the value for $F_u = 1$. It is obviously inapplicable to $F_u = 0$, i.e. to unoccupied pools. For $F_u < 1$, new correlation: $E_R = 1.3 \cdot F_u + 1.2$		
Shah (2008) analytical	$\frac{\varepsilon}{\varepsilon_0} = \frac{E}{E_0} = 3.3 \cdot U + 1$	(10)	Dependencies assuming a steady partial pressure difference. Evaporation rate for a free surface is determined according to formula (Eq. 12). Where K is a constant, defined as: $K = 35$ for $(y_a - y_{ws}) > 0.02$ or $K = 40$ for $(y_a - y_{ws}) < 0.02$ If $(y_a - y_{ws})$ is negative, its absolute value is used.		for $U < 0.1$
	$\frac{\varepsilon}{\varepsilon_0} = \frac{E}{E_0} = 1.3 \cdot U + 1.2$	(11)		for $0.1 \leq U \leq 11$	
	$\frac{\varepsilon}{\varepsilon_0} = \frac{E}{E_0} = 2.5$	(12)		for $U > 0.1$	
	$E_0 = K \cdot \rho_{ws} \cdot (\rho_a - \rho_{ws})^{1/3} \cdot (y_a - y_{ws})$	(13)			

* - The formula has been adapted to the kg/(m²·h) unit, the original symbols were changed to unify them in this article

So far, no detailed investigation results have been presented on the impact of water disturbance on the evaporation rate, as it has usually focused on the practical aspect or reference to the occupancy of an indoor pool. This study considers the influence of both warm water waves and air velocity over the surface on the evaporation rate, respectively. Experimental observations on water evaporation will be presented, assuming no additional sources of moisture around the pool surface. Investigations were carried out on the physical model of the pool surface with heated water in laboratory conditions.

2. Experimental investigation of the evaporation coefficient

2.1. Experimental setup

The test of evaporation from the disturbed water surface was conducted using an experimental facility which is located at the Faculty of Mining & Geoengineering of AGH University of Science and Technology in Cracow. The experimental facility consists of a low-velocity wind tunnel, working with a forcing fan, and a container of water equipped with both a heating system and waving-surface system located inside the test container.

The deep container made from glass with capacity of 0.09 m³ (Fig. 1) is filled with water up to the distance of 5 mm from the air inlet/outlet above the water surface. The container is of the following

dimensions: 992 mm long, 392 mm wide, 430 mm high. The air is forced through a fan with an adjustable flow rate. The mass flow rates of dry air and moisture are measured at the outlet and inlet, which allows for determining the evaporation rate of water. The essential features of the experimental apparatus are shown in Fig. 2.

The flow rates of dry air and moisture are calculated based on the recorded values of temperature and humidity, as well as the mean velocity in the cross-section of the channel. The Debimo probe for measuring the mean dynamic pressure, which allows for determining the volume of humid air, was fitted in the supply air duct. The container has a water temperature sensor, as well as a heating system. Inside the container, at the bottom, aerators, which allow for the creation of different degrees of water surface disturbance, are attached. Knowing the differences between the parameters of the supply and exhaust air from the container, an increase in moisture content was determined during the airflow over the waved water surface.

2.2. Measurement instruments

Two Rotronic AG thermo-hygrometers HC2-S were used, with a range between 5.0 and 95.0% RH (0.1% relative humidity resolution and accuracy of ±0.8%) and with a range between 0 and 50.0°C (±0.1°C resolution and accuracy), to measure the relative humidity in the inlet and outlet air.

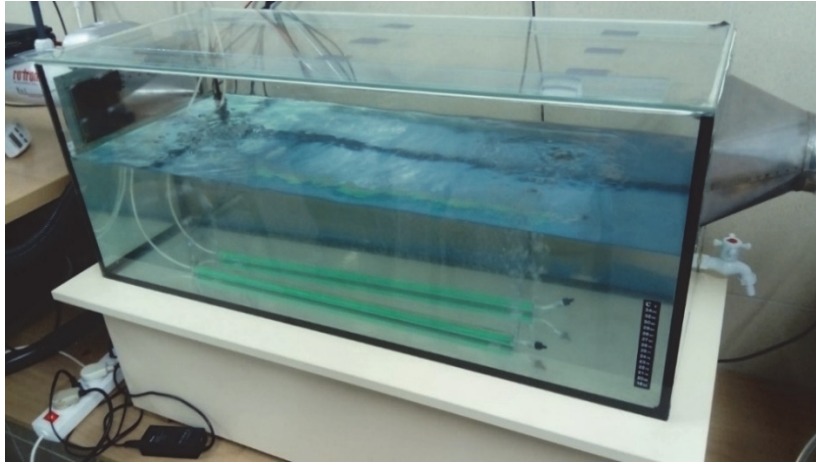
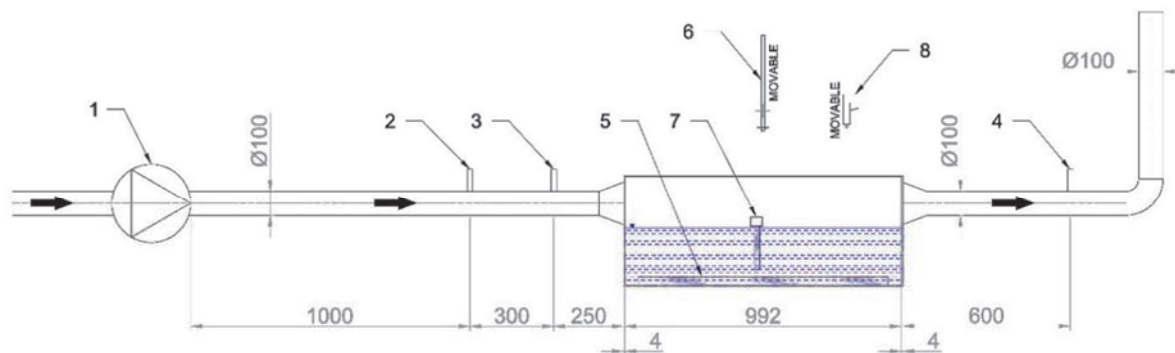


Fig. 1. View of the experimental facility



Attention: dimensions in mm

Fig. 2. Layout of the experimental facility (1 - forcing fan, 2 - dynamic pressure probe (Debimo), 3,4 - thermo-hygrometers, 5 - wave-surface generator (aerator), 6 - thermo-anemometer, 7 - water heater, 8 - infrared thermometer)

The sensor of the HC2-S probe is built on the basis of a capacitive humidity sensor made of organic polymers. Data of both dry bulb temperature and relative humidity were measured by MMod-H1-DR converter and transmitted to software APSsystem PC by RS-485 interface. Data were collected at 20 s intervals. Each measurement cycle lasted 20 minutes, and the average value of the parameters from the last minute was taken as a sample for further calculations. The probes were individually calibrated and adjusted to maximize the measurement precision before measurement investigation.

The water in the container was heated before the beginning of the test and its temperature was maintained by means of Comfort Zone Gold AQn heater with a power of 100 W. The temperature of the water surface was measured by an infrared thermometer ($\pm 0.1^\circ\text{C}$ resolution, and accuracy of $\pm 2\%$) after a 20-minute measurement cycle (measurement series). The dynamic pressure in the Debimo probe was measured thanks to Produal PEL differential pressure transducer. The accuracy of the pressure measurement from the transducer was of ± 0.5 Pa of reading and error $\pm 1\%$. The view of the board of the devices collecting measurement data is presented in Fig. 3. Software APSsystem PC reads data

from HC2-S probes by converter MMod using RS-485 interface.

It generates a graph of changes in relative humidity and air temperature over time. Fig. 4 presents changes in measured parameters during a 20-minute measurement cycle. The green curve represents relative humidity at the outlet air, while the blue one - in the inlet air. The curves of red and orange present time variability of the temperature in the inlet and outlet air, respectively.

2.3. Experimental procedure

2.3.1. Assumption of the measurement cycles

The experimental investigations were carried out for the conditions enabling obtaining similar values of the partial pressure difference. For this purpose, the same parameters were assumed between water and air before each measuring series. It allowed considering evaporation coefficient ε as a factor independent of the differential pressure. Evaporation measurements were carried out to determine the effect of the velocity and the degree of the water surface disturbance on evaporation coefficient ε . The initial assumption is to obtain such inlet air parameters that the conditions correspond at least to the turbulent free mass convection (Pauken, 1999).



Fig. 3. View of the board of devices collecting measurement data

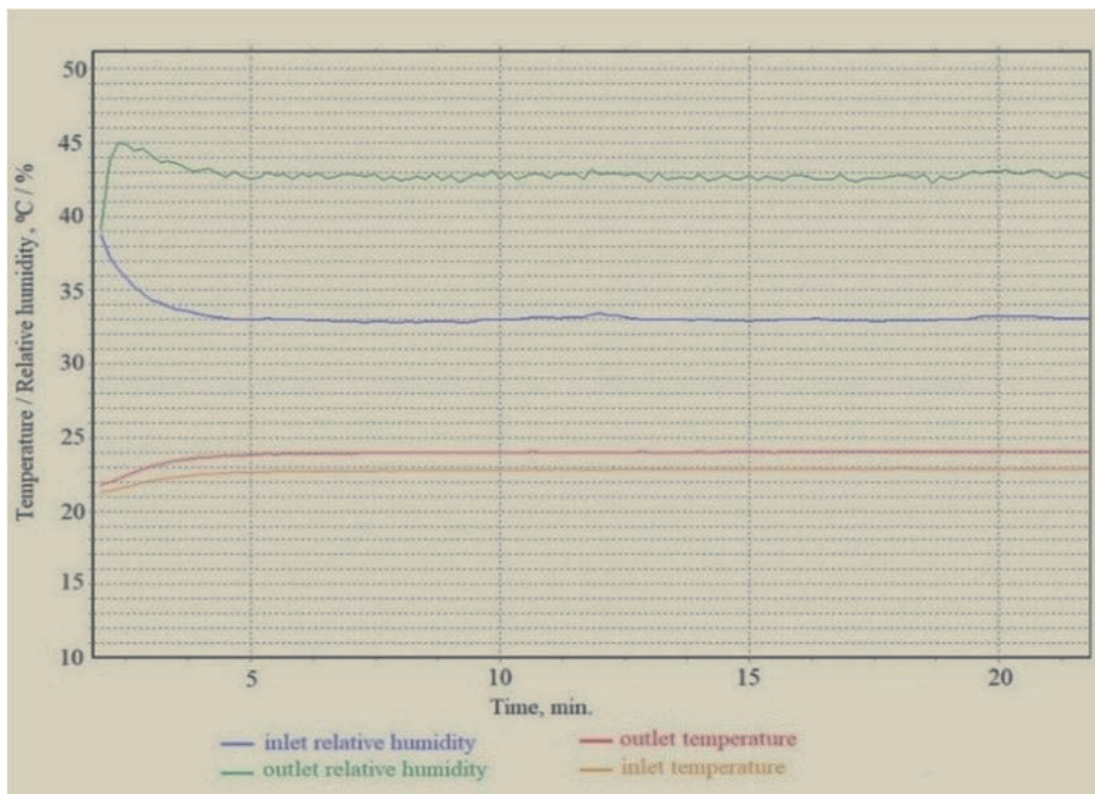


Fig. 4. Example graph of the variability of inlet and outlet air parameters plotted by AP System PC software (for λ_3 , v_{ws3} - description in the text)

Then it allows assuming the linearity of the effect of the partial pressure difference enabling the determination of evaporation coefficient ε . Experimental tests were done for 24 different conditions (measurement cycles), which include 6 mean airflow velocities over the water surface (in the range from 0.40 to 0.90 m/s) and 4 water surface disturbances ($\lambda_0, \lambda_1, \lambda_2, \lambda_3$).

Measurements were carried out in the average temperature of 26.7°C of the water surface, which was stabilised during a 20-minute time interval using the heating system, keeping the constant temperature inside the container at $27.0 \pm 0.2^\circ\text{C}$. The water surface temperature was measured before and after the finishing time of the measurement cycle, i.e. at the beginning and in the twentieth minute, respectively.

The value of temperature was assumed as the average from 10 values obtained in holes of the container's cover (cross-sections III and IV showed in Fig. 6). The value of the evaporation rate was calculated as a function of the mass flow rate of dry air and the difference in the specific humidity.

2.3.2. Inlet air parameters

Before the beginning of each measuring cycle, the parameters of the inlet air were adjusted to constant values so that they would not significantly affect the processes involved. Table 2 presents the conditions of the inlet air. The minimum and maximum values of the pressure, temperature and humidity in the inlet air stream were determined based on the recorded data. Table 2 presents the statistics of these parameters.

There was no possibility to maintain constant air parameters in the laboratory during measurement investigations. Air parameters were changing because the research was conducted in different periods of time. Barometric pressure ranged from 977.3 hPa to 992.0 hPa. Relative humidity ranged from 28.1% to 40.5%. Air temperature ranged from 21.7°C to 24.1°C.

2.3.3. Disturbance of the water surface

The disturbances of the water surface were obtained employing a performance variable aerator, which is located at the bottom of the container. The aerator consists of an air pump that draws in ambient air into two linear diffusers at the bottom of the tank. The intake air is included in the mass flow balance. The aerator's variable performance allowed for wave generation in three different ranges without producing bubbles and droplets. It allowed for simulating the disturbance of the water surface and producing water waves of various heights. The four states of mean heights of the waves were determined: 0, 1.5, 3.0 and 5.0 mm, respectively. The first one (0 mm) corresponds to the free water surface. The three remaining states were determined in proportion to the capacity of the aerator.

The maximum state of disturbed water surface (5.0 mm) corresponded to the highest possible spatter-free wave, which means that the drops were not carried away by the air stream flowing over its surface (Fig. 5). The wave height was related to the length of the characteristic airflow over the water L (related to the width of the surface), and disturbance index $\lambda = h/L$ was developed. Three disturbance indices were measured: $\lambda_1 = 0.015$, $\lambda_2 = 0.030$, $\lambda_3 = 0.050$, respectively.

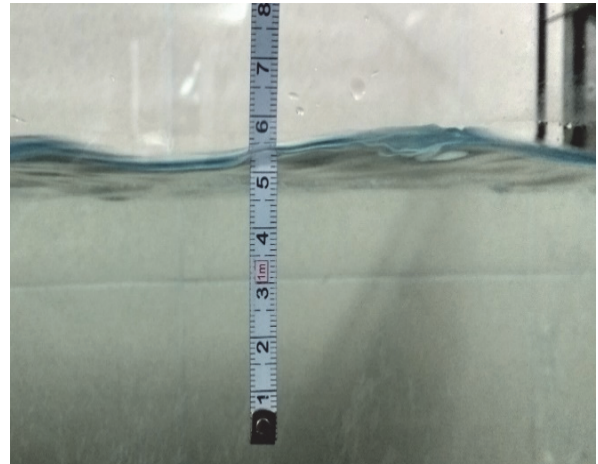


Fig. 5. View of the wave height measurement ($\lambda_3 = 0.050$)

2.3.4. Air velocity over the water surface

Air flow was determined using the forcing fan speed controller. The velocity of the air above the water surface was measured employing the thermo-anemometer for the free water surface. For this purpose, an additional cover of the container was made with thirty measurement points, arranged according to Fig. 6.

The thermo-anemometer was placed in a given hole at the distance of 5 mm above the water surface with the remaining holes closed. The measurements were carried out for each of the six-volume streams of air supply by the fan in order to guarantee different air velocities above the water surface.

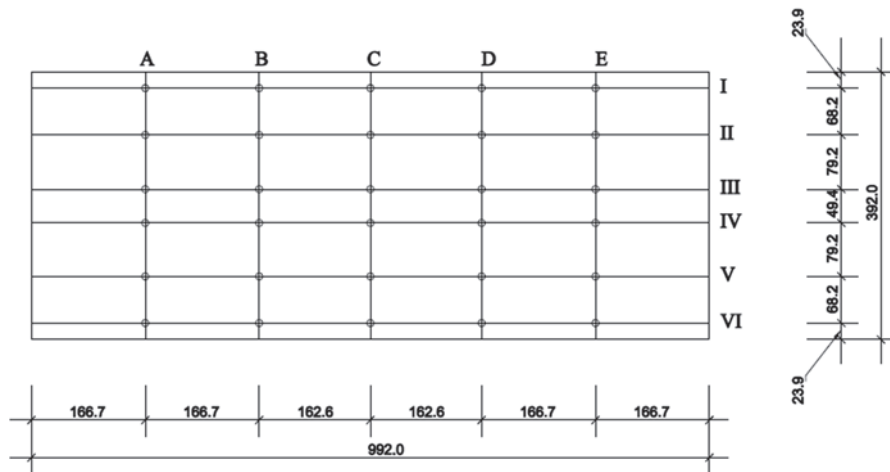


Fig. 6. Location of measuring holes in the container's cover

It was assumed that the air velocity over the water surface is constant for a given fan setting, and the water surface disturbance does not affect its value. To determine the average velocity, the Kriging method of estimating results was used. The average air velocity over the water surface was determined as the arithmetic means of all the data taken at a distance of 5.0 mm from the water surface. Fig. 7 presents the isotachs over the water surface for the average value of 0.40 m/s.

For the analysis of the changes in the evaporation rates, four test-cases, with air velocities over the water surface: $v_{ws1} = 0.40$ m/s, $v_{ws2} = 0.51$ m/s, $v_{ws3} = 0.59$ m/s, $v_{ws4} = 0.66$ m/s, $v_{ws5} = 0.81$ m/s, $v_{ws6} = 0.93$ m/s, respectively, were chosen.

3. Analysis of the experimental data

3.1. Results of evaporation coefficients measurements

The results obtained from the last 10 minutes of the variable measurement cycles allowed to calculate the mass flow rate of evaporated water, respectively flowing out and flowing in. It was

calculated as the product of the specific humidity difference and the mass rate of dry air. The values of evaporation rates were determined from the transformation of dependencies (Eqs. 2-3). The results are provided in Appendix 1. It can be seen that evaporation values have not changed in time range from the tenth to the twentieth minute. Also, partial pressures of both water vapour above the water and at the inlet air were not changing significantly during different cycles of the experiment.

The minimum and maximum average values of the pressure difference in measurement cycles were 2549 Pa and 2572 Pa, respectively. For further purposes, the assumption of the stability of the differential partial pressure at 2557 Pa in all the measuring cycles can be assumed. The latent heat of vaporization of the surface water (h_w) for the temperature of 26.7°C is 2439 kJ/kg. This assumption allowed to determine evaporation coefficient ε for every condition investigated.

For further analysis, the average values for various air velocities and various heights of the waved water surface were determined, and are summarized in Table 2.

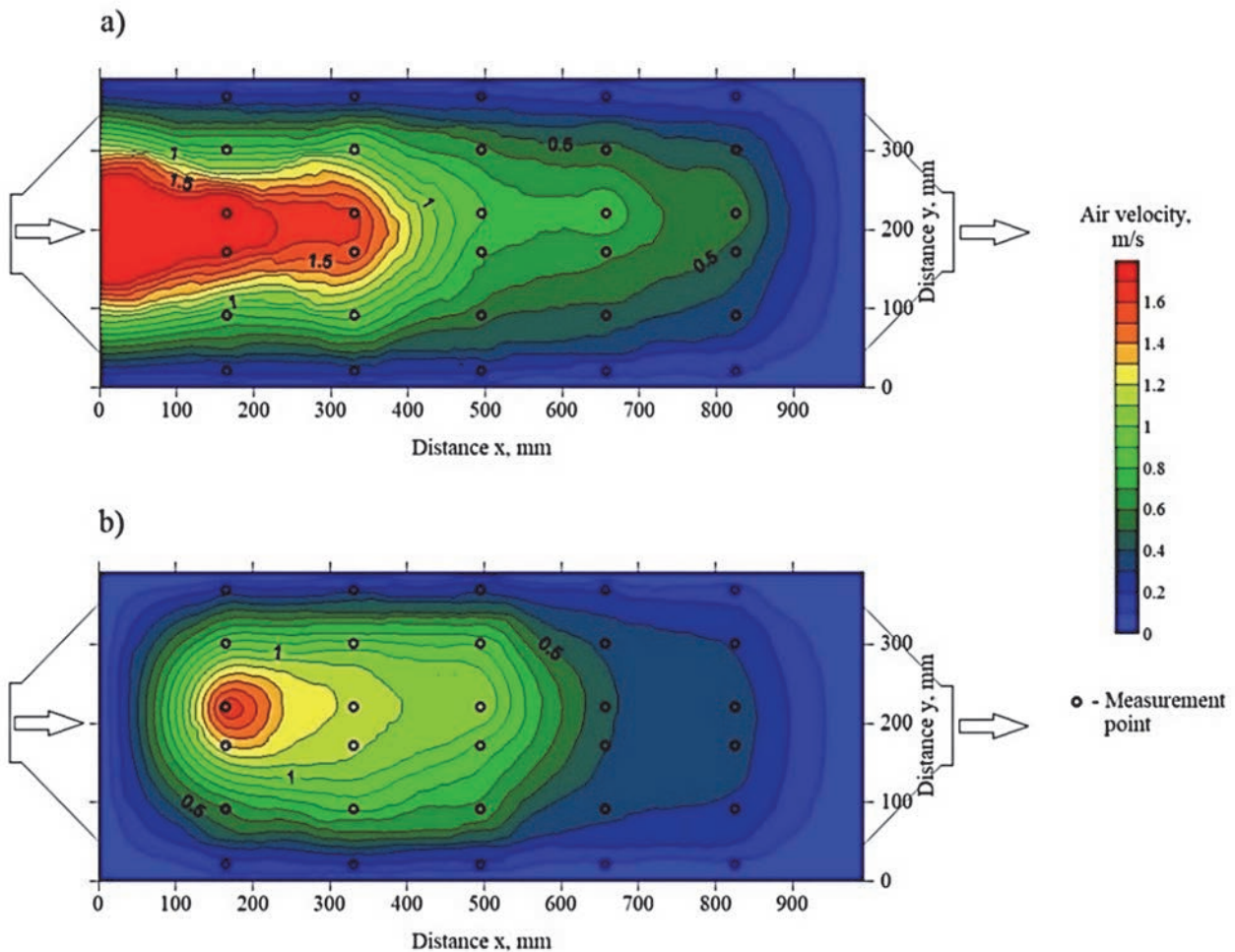


Fig. 7. Air velocity distribution over the water surface ($v_{ws} = 0.40$ m/s) - horizontal projection, a) in the plane passing through the duct axis; b) for a distance of 5.0 mm above the water surface

Table 2. Average values of evaporation coefficient ε for various cycles of the experiment

v_{ws}	λ_0	λ_1	λ_2	λ_3
m/s	$\varepsilon_0, \text{g}/(\text{m}^2 \cdot \text{Pa} \cdot \text{h})$	$\varepsilon_1, \text{g}/(\text{m}^2 \cdot \text{Pa} \cdot \text{h})$	$\varepsilon_2, \text{g}/(\text{m}^2 \cdot \text{Pa} \cdot \text{h})$	$\varepsilon_3, \text{g}/(\text{m}^2 \cdot \text{Pa} \cdot \text{h})$
0.4	0.179	0.202	0.226	0.243
0.51	0.243	0.268	0.277	0.294
0.59	0.269	0.280	0.289	0.318
0.66	0.303	0.324	0.339	0.355
0.81	0.348	0.373	0.380	0.408
0.93	0.408	0.427	0.451	0.465

3.2. Discussion

3.2.1. Impact of air velocity over the water surface

Fig. 8 shows the changes in evaporation coefficient ε as functions of air flow velocity. It can be seen that the calculation results of evaporation coefficients ε based on the experimental data form a straight line according to the air velocity over the water surface. The parallel shift of the linear function depending on the increase in wave height is also visible. An increase in water surface disturbance does not disrupt the linearity of this dependencies, which can be obtained by curve fitting to the test data by regression (Eq. 14):

$$\varepsilon = f(v_{ws}) = a \cdot v_{ws} + b \tag{14}$$

when using linear regression, the slope of linear function $a = 0.41$ was determined.

It can be seen that coefficient b is dependent on the degree of the water surface disturbance due to the visible course of the parallel fitted lines.

3.2.2. Comparison of experimental results with models of free or forced convection effects

The experimental results were obtained for the

air velocity ranging from 0.40 to 0.90 m/s. Ventilation of indoor pools is usually designed for air velocity over the floor, which does not exceed 0.15 m/s (Shah, 2018). Most of the empirical formulas for water evaporation in pool halls are appropriate for speed range from 0.05 to 0.10 m/s, which corresponds to the predominance of the free convection effect. Free convection plays a more significant role, and the effects of forced convection are weaker in this range. The air velocity in the analysed range should not affect evaporation. With an increase in air velocity over the saturated layer over the free water surface, the advection mechanism becomes more and more relevant. Usually, in the case of air velocities above 0.15 m/s (or above 0.20 m/s for specific conditions), the predominance of forced convection in the evaporation of water should be taken into account (Shah, 2018). The effect of forced convection becomes dominant, though still, molecular motion cannot be totally neglected. According to Pauken (1999) and Blázquez et al. (2017) studies, the limits of the mixed convective range are determined by dimensionless product Gr_m / Re_L^2 . For the mixed convective range, this product should be in the range of $0.1 < Gr_m / Re_L^2 < 5.0$.

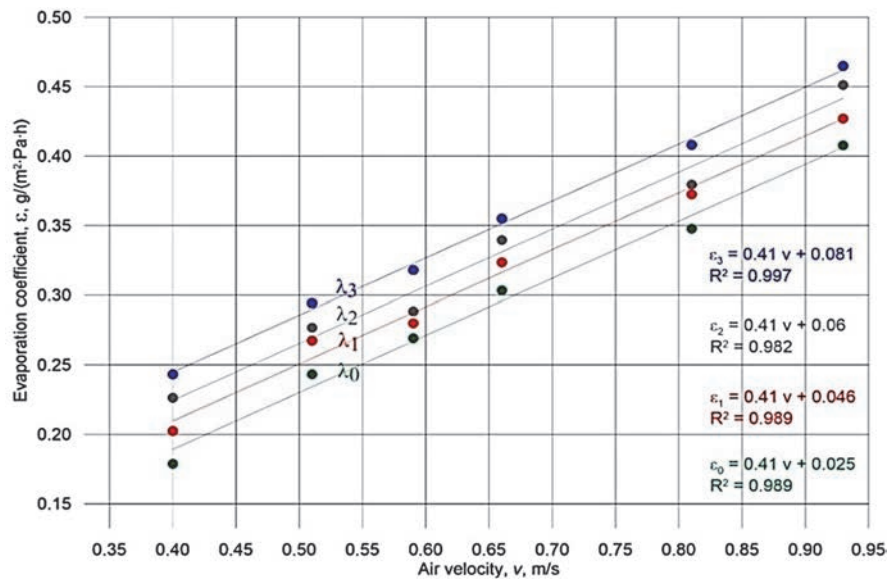


Fig. 8. Evaporation coefficient ε as a function of air velocity over the water surface $\varepsilon = f(v_{ws})$ for water temperature $t_{ws} = 26.7^\circ\text{C}$ and various surface disturbances λ

Under experimental conditions, this range corresponds to the range of air velocity from 0.195 to 1.45 m/s. The measurement results obtained relate to Reynolds number range of $2.63 \cdot 10^4$ to $6.11 \cdot 10^4$, based on the characteristic length of water surface. The mass-based Gasthof number ranged from $6.03 \cdot 10^8$ to $9.46 \cdot 10^8$. Thus, the experiments conducted in this investigation are in the range of $0.16 < G_{rm} / Re_L^2 < 1.3$.

As previously stated, many of the experimental models make the value of the evaporation rate dependent on the air velocity over the free water surface, presenting the relationship in the form of a

linear function. Table 3 presents the formulas which were used to compare the new formula obtained from the experimental investigations. Fig. 9 shows the dotted line according to the new formula for a free water surface against the background of other authors' evaporation models. Fig. 9 was created for the range of mixed convection under experimental conditions.

The steepness of the straight line for the free water surface is higher than the rest of the plotted lines, which results from the higher temperature difference between water and air under experimental conditions than in other studies.

Table 3. Various correlations for the determination of evaporation coefficient ε

Author	Correlation of evaporation coefficient ε $kg/(m^2 \cdot Pa \cdot h)$	Note
Himus and Hinchley (1924)	$\varepsilon_0 = 3600 \cdot (64.58 + 28.06 \cdot v_{ws}) \cdot 10^{-6}$ (15)	Investigations with relatively small pans having surface areas in the order $0.02 \pm 0.07 \text{ m}^2$ and with high turbulent conditions.
Rowher (1931)	$\varepsilon_0 = 3600 \cdot (64.72 + 20.97 \cdot v_{ws}) \cdot 10^{-6}$ (16)	Wind tunnel with evaporation pan (0.84 m^2)
Malicki (1962)	$\varepsilon_0 = 1000 \cdot (0.022 + 0.0174 \cdot v_{ws}) \cdot \frac{760}{p}$ (17)	for $t_a < 30^\circ\text{C}$ and for $t_{ws} < 40^\circ\text{C}$
Shah (2014)	$\varepsilon_0 = 0.05 \cdot \left(\frac{v_{ws}}{0.15}\right)^{0.7}$ (18)	For velocity greater than 0.15 m/s
Raimundo et al. (2014)	$\varepsilon_0 = 0.0036 \cdot (37.17 + 32.19 \cdot v_{ws})$ (19)	Investigation carried out in the range of partial pressure differences 1850-8751 Pa at air velocity in the range from 0.101 to 0.697 m/s.
Shah (2018)	$\varepsilon_0 = 0.05 \cdot \left(\frac{v_{ws}}{0.12}\right)^{0.8}$ (20)	Model validated from 0.02 to 525 m^2 , water temperatures from 7°C to 94°C , air temperatures from 6°C to 51°C , relative humidity from 16% to 98%, and air velocity up to 1.90 m/s.

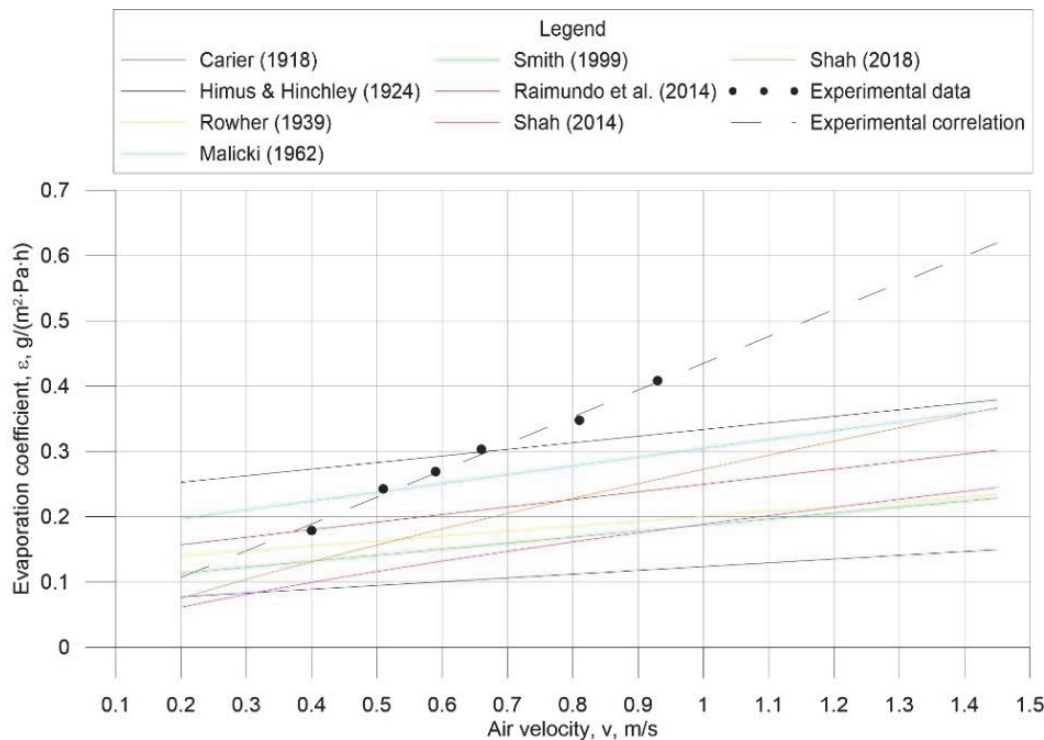


Fig. 9. Comparison of evaporation coefficient ε as a function of air velocity over the free water surface for various correlations (case without water surface disturbances)

3.3. Effect of water surface disturbance

The obtained experimental results show that according to expression (Eq. 14), coefficient b_i of the linear regression of water transfer coefficient ε depends on water surface disturbance, $b = f(\lambda)$.

The coefficient b varies from 0.025 for free water surface to 0.081 for a very rough surface with the same temperature difference 1.5°C at the air-water interface. The results show that the total surface roughness (λ_3) causes a 3.2-fold increase in coefficient b than from the undisturbed water surface. The experimentally determined evaporation coefficients refer to the different levels of water surface disturbances. Until now, the effect of spatter-free wave height (without the splashing of water) on evaporation has not been studied. Most investigators have focused on the practical factor of the increase in water evaporation so far, which is the surface pool occupancy. The comparison of their investigations and the effect of water surface disturbance have been made in the article. Most researchers determine evaporation rate as dependent on a type of the pool or a number of occupants, which is a practical approach to the issue. The comparison of the evaporation rate at different heights of the water wave to the occupancy will allow for the verification of the test results obtained.

According to Smith et al. (1998) the evaporation rate for occupied pools is characterized by evaporation ratio E_R , which compares the evaporation rate during the occupancy of the pool to the evaporation from an inactive pool in the same conditions. The authors presented the evaporation ratio E_R as a function of a number of people per surface and proposed relation (Eq. 7) in Table 1.

Since an increase in the evaporation rate is a linear function of occupancy and an increase in the evaporation rate due to wave size is also a linear function, it is possible to compare these two relationships. Assuming the stability of water vapour pressure difference Δp , the following expression can also be used to compare the evaporation rate results for different water wave sizes with a number of people, according to formula (Eq. 7) in Table 1.

On the basis of the test result obtained, ratio $\varepsilon/\varepsilon_0$ for each of the analyzed water surface disturbances is determined. For a free convection effect, the air velocity in the analyzed range should not significantly affect the evaporation. According to the

investigations of Pauken (1999) and Blázquez et al. (2017), the influence of the forced convection effect is neglected when $Gr_m/Re_L^2 > 5.0$, which under the conditions of the experiment corresponds to air velocity $v_{init} < 0.195$ m/s. For further calculations, the ratio of evaporation coefficients $\varepsilon/\varepsilon_0$ for the initial air velocity value of 0.195 m/s is assumed. The air velocity above this value does not significantly change the ratio of coefficients $\varepsilon/\varepsilon_0$.

Table 4 presents the calculation results of ratio $\varepsilon/\varepsilon_0$ for three examined wave heights ($\lambda_1, \lambda_2, \lambda_3$). The error that is made assuming this initial velocity for the disturbed water surface for ($\lambda_1, \lambda_2, \lambda_3$) is 4, 6 and 21%, respectively.

Table 4. Ratio of evaporation coefficients $\varepsilon/\varepsilon_0$ for initial air velocity value

$v_{init}, \text{ m/s}$	$\varepsilon_1 / \varepsilon_0$	$\varepsilon_2 / \varepsilon_0$	$\varepsilon_3 / \varepsilon_0$
0.195	1.200	1.333	1.534

The experimental results obtained refer to three ranges of water disturbance (wave sizes), ($\lambda_1, \lambda_2, \lambda_3$), which can be applied to a number of occupants per unit pool area. The test variant with undisturbed water surface (λ_0) can be related to unoccupied pools. According to the methodology presented by Smith (1998) and Shah (2014), the range of a wave size during the experiment shows an increase in the evaporation rate according to the function of the linear coefficient of occupancy N^* . Thus, coefficient b_i of the linear function (Eq. 14) depends on the disturbances of water surface, and therefore it is directly proportional to ratio $\varepsilon/\varepsilon_0$.

$$\frac{\varepsilon}{\varepsilon_0} = b = b_0 \cdot (c \cdot N^* + d) \quad (21)$$

Occupancy N^* can be calculated for three studied wave sizes: ($\lambda_1, \lambda_2, \lambda_3$) by substituting the formula (Eq. 14) to (Eq. 21). On that basis, the linear relationship between coefficient b and coefficient of occupancy N^* is obtained. The results are shown in Table 5. The approximation of function (Eq. 21) to the results is shown in Fig.10. The value of coefficient b_0 is 0.025 according to the results obtained for λ_0 . Coefficients c and d in the formula (Eq. 21) were determined based on the linear regression of ratios $\varepsilon/\varepsilon_0$ and N^* .

Table 5. Calculation results of coefficient of occupancy N_i^* related to investigated water surface disturbances

Wave size	Average ratio $\varepsilon / \varepsilon_0, -$	Coefficient b acc. to formula (Eq. 21)	Coefficient of occupancy N_i^* , person/m ²
λ_0	1.000	0.031	0
λ_1	1.200	0.057	0.038
λ_2	1.333	0.075	0.069
λ_3	1.534	0.101	0.116

Taking into account relations (Eq. 7) and (Eq. 21), water transfer coefficient ε can be presented in the following form: (Eq. 22), provided that there should be at least 4.6 m² of water surface per person. The results of ε calculations for three wave sizes during the experiment were compared to other models based on N^* use.

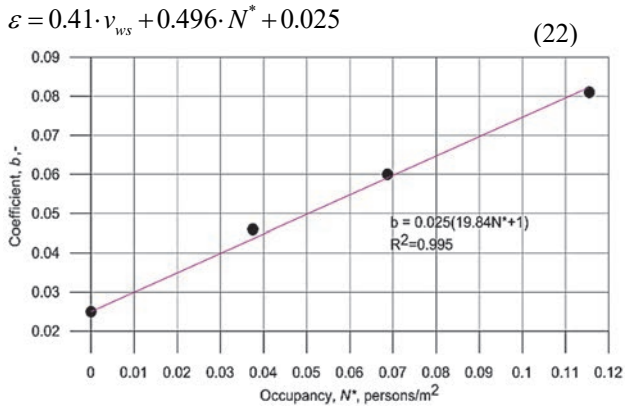


Fig. 10. Coefficient b as a function of coefficient of occupancy N^*

In addition to the Smith (1998) model, the models of Biasin and Krumme (1974) and Hens (2009), and Shah (2008, 2018) were used for comparison results. In the model given by Shah (2018), a correction factor depending on utilization factor U was taken into account. Fig. 11 presents the results of the calculations. Evaporation coefficient ε_i obtained according to formula (Eq. 22) is comparable with the formulas given by Smith et al. (1998) and Shah (2008, 2018).

4. Calculation example of a thermal pool–practical significance

To illustrate the method for determining water evaporation, an example of a real object was used. The

evaporated water mass was calculated for a thermal pool with dimensions of 10x20x1.5m. The temperature of 26.0°C and relative humidity of 40% in indoor air are considered, respectively.

The mean velocity of the air above the waved water surface is 0.20 m/s. The water vapour partial pressure in the air is 1353 Pa. The water surface temperature is 30°C, which corresponds to the partial pressure of saturated vapour of 4242 Pa. The moisture transfer is associated not only with water evaporation from the spatter-free waved surface. For instance, it may correspond to a thermal swimming pool, in which 20 people move slowly and create a small water wave. Occupancy factor is $N^* = 0.1$ persons/m², and it is close to water surface disturbance λ_3 during the experiment.

Knowing the surface of the water basin and the difference in parameters at the water-air interface, evaporation coefficient ε was determined, which is 0.157 g/(m²·Pa·h), according to relation (Eq. 22). The results were compared to other methods that differentiate the evaporation rate depending on a type and purpose of an indoor pool. Fig. 12 shows the results of this comparison. According to the experimental correlation proposed, the evaporation rate is 90.5 kg/h, which corresponds to a unit evaporation of 0.452 kg/(m²·h). A large discrepancy in the results of the calculations of the evaporation rate can be noticed while analysing the results obtained. Correlation VDI-1 should be rejected because of its purpose for free water surface, as well as VDI-4 due to their use for evaporation calculation from the water surface, including splashes.

The experimental correlation for the conditions assumed is the closest to the correlations, which does not take into account the influence of air velocity, i.e. VDI-2. From the correlations which take into account the influence of air velocity and occupancy, the result is closest to ASHRAE (2015)-5 formula, the correlation of Smith et al. (1998) and the analytical Shah's (2003) correlation. ASHRAE formula (2015)-5 includes activity factor $F_u=1.0$, but not occupancy.

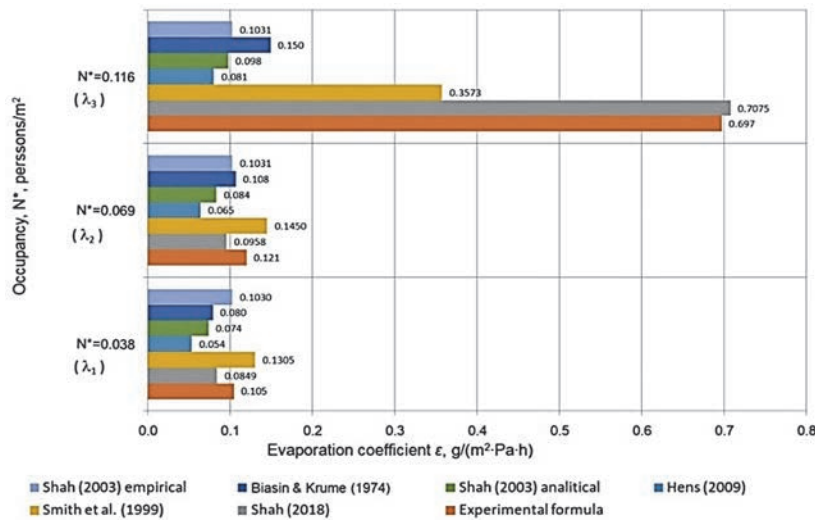


Fig. 11. Comparison of evaporation coefficient ε according to various methods depending on coefficient of occupancy

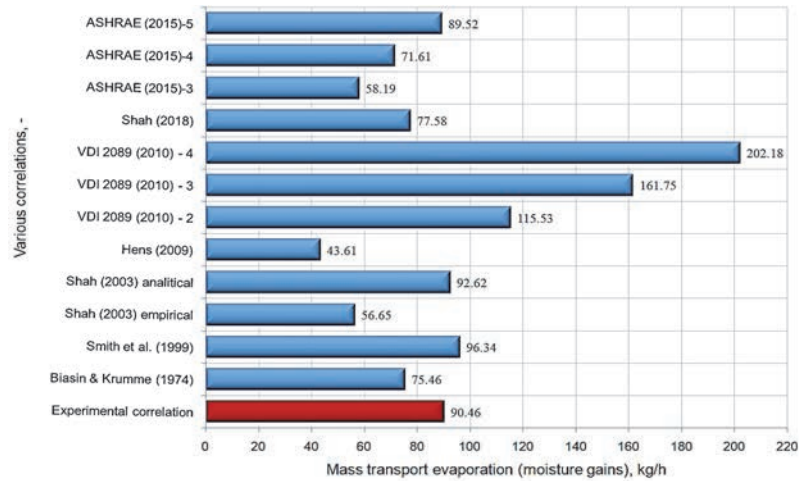


Fig. 12. Comparison of the evaporation rate for the thermal pool according to different correlations

Therefore, the relationship proposed can only be compared to Smith's (Smith et al. 1998) correlation and to Shah's (2003) correlation, respectively. The evaporation rate based on experimental correlation is about 15% higher than Smith's and about 17% of Shah's correlations. Due to both heat and mass transfer to the air as a result of the temperature difference of 4.0°C at the water-air interface, this result is higher than the one from other correlations.

5. Conclusions

Water evaporation rate from a pool depends, among others, on the water surface disturbance and the velocity of the air stream over the water surface. The results of the evaporation rates obtained from the experimental setup with variables of both disturbances of heated water surface and air velocities enabled the determination of the evaporation coefficients for the temperature difference at the water-air interface for conditions in which forced convection dominates.

The new formula for the prediction of evaporation coefficient was developed based on the experimental results obtained. Formula was expanded to the range of the mixed convection, i.e. for both fully turbulent and transition regimes, which refers to air velocity range from 0.20 to 1.45 m/s under the experimental conditions.

The experimental results confirm the results of other investigators that the evaporation rate for the constant vapour pressure differential increases linearly with air velocity over the water surface. The slope of the linear function (directional coefficient of the straight line) does not depend on the size of water surfaces disturbance when the water and ambient parameters do not change. The increment of the evaporation coefficient as a function of air velocity is nearly identical to Smith's and Shah's correlations.

The size of the water surface disturbance makes the linear function graph shift in a parallel way.

As far as the engineering approach is concerned, the height of the water wave was compared

in experiments to the use of occupancy factor N^* . The highest water wave in the experimental setup, i.e. $\lambda_3 = 0.030$, corresponds to occupancy coefficient $N^* = 0.116$, which is related to water surface area 8.7 m²/per person. It can be assumed that the evaporation rate depends linearly on the occupancy factor and the velocity of the air stream for both conditions, spatter-free water waves and the lack of other sources of water evaporation.

The empirical correlation proposed in this study is based on the measurements of water evaporation from a small water surface with temperature 26.8°C to the air stream with temperature of 23.7°C. Hence, its application is also restricted to the prediction of the water evaporation rate from small pools such as: small therapeutic pools, thermal baths, tanks, containers and other vessels containing warm water. It can be applied to air velocity over the water surface in the range from 0.20 to 1.40m/s. The issue of the relationship of the heat transfer with the roughness of water body surface has not been studied in this experiment, and needs further investigation.

The empirical correlation developed is used mainly for the qualitative assessment of the impact of both air velocity over waved water surface in basins and reservoirs with artificially heated water. The results obtained may be helpful in engineering practice or may be used to validate CFD models in the field of experimental investigation.

Nomenclature

- a, b – coefficients of empirical equation in (Eq. 14);
- A_{ws} – surface of evaporating water, m²;
- c, d – coefficients of empirical equation in (Eq. 22);
- E – evaporation rate for disturbed water's surface, kg/(m²·h);
- E_0 – evaporation rate for free surface (unoccupied pool), kg/(m²·h);
- E_R – evaporation ratio, kg/(m²·h);
- F_a – activity factor (acc. to ASHRAE), -;

F_u – pool utilization factor (activity factor), -;
 Gr_m – mass-based Grashoff number, -,
 $Gr_m = \frac{\rho \cdot (\rho_a - \rho_i) \cdot g \cdot L^3}{\mu^2}$;
 h_e – evaporative heat transfer coefficient, W/(m²·Pa);
 h_w – latent heat of vaporization of water, J/kg, kJ/kg;
 K – constant of Shah’s in (Eq. 13),-;
 \dot{m}_{H_2O} – mass flow rate of evaporated water, kg/h;
 N – number of occupants, -;
 N^* – coefficient of occupancy, $N^* = N / A$, 1/m²;
 p – barometric pressure, Pa;
 p_a – water vapour partial pressure at air temperature and humidity, Pa;
 p_{ws} – saturated water vapour partial pressure at water surface temperature, Pa;
 Re_L – Reynolds number, -, $Re_L = \frac{v_{ws} \cdot L}{\nu}$;
 t_{ws} – water surface temperature, °C;
 U – utilization factor, $U = 4,5 \cdot N^*$, -;
 v_{ws} – velocity of air stream moving over water surface, m/s;
 y_a – specific air humidity, kg of moisture/kg of air;
 y_{ws} – specific humidity of saturated air over plane surface of pure water at temperature t_{ws} , kg of moisture/kg of air.

Greek letters

λ – water surface disturbance index (av. height of water wave to characteristic length of water surface, $\lambda = h / L$, -;
 β – activity factor (acc. to VDI 2089)
 ε_0 – evaporation coefficient based on the difference in vapour pressures above free water surface and ambient air, kg/(m²·Pa·h);
 ε – evaporation coefficient based on the difference in vapour pressures above disturbed water surface and ambient air, kg/(m²·Pa·h);
 ρ – air density based on average film temperature at water-air interface, kg/m³;
 ρ_a – air density, kg/m³;
 ρ_i – air density at the interface at 100% saturation, kg/m³;
 ρ_a – air density, kg/m³;
 ρ_{ws} – air density of saturated vapour over the water surface, kg/m³;
 μ – dynamic viscosity of air, Pa·s;
 ν – kinematic viscosity of air, m²/s.

Subscripts

0 – for parameters related to free water surface,
 1, 2, 3, ... – for parameters related to disturbed water surface,
 init. – initial conditions.

Appendix 1. Results of water evaporation measurements

v_{ws} m/s	t min	$\lambda=0$				$\lambda=0,015$				$\lambda=0,03$				$\lambda=0,05$			
		$\dot{m}_{i,0}$ kg/h	p_{a0} Pa	p_{ws0} Pa	E_0 kg/(m ² ·h)	$\dot{m}_{i,0}$ kg/h	p_{a1} Pa	p_{ws1} Pa	E_1 kg/(m ² ·h)	$\dot{m}_{i,0}$ kg/h	p_{a2} Pa	p_{ws2} Pa	E_2 kg/(m ² ·h)	$\dot{m}_{i,0}$ kg/h	p_{a3} Pa	p_{ws3} Pa	E_3 kg/(m ² ·h)
0.40	10	0.173	941	3502	0.445	0.197	958	3523	0.508	0.219	946	3481	0.562	0.239	946	3502	0.613
	11	0.165	943	3481	0.425	0.192	935	3502	0.494	0.231	932	3502	0.594	0.236	941	3523	0.607
	12	0.163	946	3523	0.418	0.197	944	3523	0.506	0.223	935	3502	0.574	0.214	938	3502	0.550
	13	0.173	960	3502	0.446	0.197	958	3502	0.508	0.225	946	3502	0.579	0.253	949	3523	0.650
	14	0.181	952	3502	0.465	0.197	941	3502	0.507	0.222	935	3523	0.570	0.238	935	3502	0.612
	15	0.185	941	3523	0.477	0.200	952	3523	0.513	0.224	943	3502	0.576	0.236	940	3502	0.607
	16	0.172	955	3502	0.443	0.202	943	3502	0.519	0.221	935	3502	0.568	0.244	958	3502	0.627
	17	0.185	952	3481	0.475	0.195	964	3481	0.502	0.223	949	3502	0.572	0.249	935	3523	0.640
	18	0.183	949	3502	0.470	0.206	955	3502	0.531	0.233	946	3481	0.598	0.217	961	3481	0.557
	19	0.185	964	3502	0.477	0.207	964	3523	0.531	0.226	949	3502	0.582	0.244	958	3523	0.628
0.51	10	0.186	964	3502	0.479	0.205	964	3523	0.527	0.238	949	3502	0.612	0.249	958	3523	0.640
	10	0.225	943	3502	0.578	0.275	938	3523	0.706	0.272	949	3502	0.700	0.270	978	3523	0.695
	11	0.244	938	3502	0.627	0.276	938	3502	0.709	0.276	932	3502	0.709	0.268	941	3523	0.689
	12	0.248	955	3481	0.639	0.281	944	3523	0.723	0.270	935	3502	0.694	0.300	941	3481	0.771
	13	0.246	958	3502	0.632	0.275	952	3502	0.707	0.270	949	3502	0.694	0.301	952	3523	0.774
	14	0.239	952	3543	0.615	0.254	949	3502	0.654	0.277	935	3523	0.712	0.300	935	3502	0.773
	15	0.245	944	3523	0.631	0.246	958	3523	0.632	0.282	972	3523	0.726	0.300	946	3502	0.771
	16	0.253	955	3502	0.650	0.252	946	3502	0.648	0.264	952	3481	0.678	0.288	952	3481	0.741
	17	0.243	958	3481	0.625	0.254	970	3481	0.653	0.271	967	3502	0.696	0.284	984	3523	0.730
	18	0.229	955	3502	0.589	0.262	955	3502	0.673	0.278	935	3481	0.715	0.309	969	3543	0.795
0.59	19	0.243	946	3523	0.624	0.263	969	3543	0.676	0.284	952	3502	0.730	0.302	949	3523	0.777
	20	0.246	943	3502	0.631	0.258	972	3523	0.664	0.288	949	3502	0.740	0.297	944	3502	0.764
	10	0.273	943	3502	0.701	0.286	946	3564	0.736	0.323	949	3502	0.831	0.340	978	3543	0.876
	11	0.277	932	3481	0.712	0.291	935	3523	0.749	0.321	932	3523	0.825	0.316	946	3543	0.812
	12	0.266	958	3543	0.684	0.281	949	3523	0.724	0.287	938	3502	0.738	0.316	944	3481	0.812
	13	0.267	935	3502	0.687	0.281	952	3502	0.723	0.296	949	3502	0.761	0.316	955	3543	0.812
	14	0.271	952	3543	0.698	0.278	949	3502	0.716	0.278	935	3523	0.714	0.315	935	3502	0.809
	15	0.265	952	3523	0.680	0.276	958	3481	0.709	0.283	972	3502	0.728	0.296	946	3543	0.761
	16	0.267	961	3502	0.686	0.277	943	3502	0.713	0.27	952	3481	0.694	0.305	955	3502	0.785
	17	0.260	958	3481	0.670	0.268	970	3481	0.688	0.27	961	3502	0.695	0.333	984	3523	0.857
18	0.269	952	3502	0.693	0.280	955	3502	0.720	0.288	935	3481	0.741	0.302	969	3543	0.777	
19	0.264	946	3502	0.678	0.263	972	3481	0.677	0.271	952	3502	0.698	0.321	955	3543	0.826	
20	0.266	943	3481	0.683	0.273	969	3481	0.702	0.266	952	3502	0.684	0.338	949	3543	0.869	

0.66	10	0.173	941	3502	0.445	0.197	958	3523	0.508	0.219	946	3481	0.562	0.239	946	3502	0.613
	11	0.165	943	3481	0.425	0.192	935	3502	0.494	0.231	932	3502	0.594	0.236	941	3523	0.607
	12	0.163	946	3523	0.418	0.197	944	3523	0.506	0.223	935	3502	0.574	0.214	938	3502	0.550
	13	0.173	960	3502	0.446	0.197	958	3502	0.508	0.225	946	3502	0.579	0.253	949	3523	0.650
	14	0.181	952	3502	0.465	0.197	941	3502	0.507	0.222	935	3523	0.570	0.238	935	3502	0.612
	15	0.185	941	3523	0.477	0.200	952	3523	0.513	0.224	943	3502	0.576	0.236	940	3502	0.607
	16	0.172	955	3502	0.443	0.202	943	3502	0.519	0.221	935	3502	0.568	0.244	958	3502	0.627
	17	0.185	952	3481	0.475	0.195	964	3481	0.502	0.223	949	3502	0.572	0.249	935	3523	0.640
	18	0.183	949	3502	0.470	0.206	955	3502	0.531	0.233	946	3481	0.598	0.217	961	3481	0.557
	19	0.185	964	3502	0.477	0.207	964	3523	0.531	0.226	949	3502	0.582	0.244	958	3523	0.628
20	0.186	964	3502	0.479	0.205	964	3523	0.527	0.238	949	3502	0.612	0.249	958	3523	0.640	
0.81	10	0.225	943	3502	0.578	0.275	938	3523	0.706	0.272	949	3502	0.700	0.270	978	3523	0.695
	11	0.244	938	3502	0.627	0.276	938	3502	0.709	0.276	932	3502	0.709	0.268	941	3523	0.689
	12	0.248	955	3481	0.639	0.281	944	3523	0.723	0.270	935	3502	0.694	0.300	941	3481	0.771
	13	0.246	958	3502	0.632	0.275	952	3502	0.707	0.270	949	3502	0.694	0.301	952	3523	0.774
	14	0.239	952	3543	0.615	0.254	949	3502	0.654	0.277	935	3523	0.712	0.300	935	3502	0.773
	15	0.245	949	3523	0.631	0.246	958	3523	0.632	0.282	972	3523	0.726	0.300	946	3502	0.771
	16	0.253	955	3502	0.650	0.252	946	3502	0.648	0.264	952	3481	0.678	0.288	952	3481	0.741
	17	0.243	958	3481	0.625	0.254	970	3481	0.653	0.271	967	3502	0.696	0.284	984	3523	0.730
	18	0.229	955	3502	0.589	0.262	955	3502	0.673	0.278	935	3481	0.715	0.309	969	3543	0.795
	19	0.243	946	3523	0.624	0.263	969	3543	0.676	0.284	952	3502	0.73	0.302	949	3523	0.777
20	0.246	943	3502	0.631	0.258	972	3523	0.664	0.288	949	3502	0.74	0.297	944	3502	0.764	
0.93	10	0.273	943	3502	0.701	0.286	946	3564	0.736	0.323	949	3502	0.831	0.340	978	3543	0.876
	11	0.277	932	3481	0.712	0.291	935	3523	0.749	0.321	932	3523	0.825	0.316	946	3543	0.812
	12	0.266	958	3543	0.684	0.281	949	3523	0.724	0.287	938	3502	0.738	0.316	944	3481	0.812
	13	0.267	935	3502	0.687	0.281	952	3502	0.723	0.296	949	3502	0.761	0.316	955	3543	0.812
	14	0.271	952	3543	0.698	0.278	949	3502	0.716	0.278	935	3523	0.714	0.315	935	3502	0.809
	15	0.265	952	3523	0.680	0.276	958	3481	0.709	0.283	972	3502	0.728	0.296	946	3543	0.761
	16	0.267	961	3502	0.686	0.277	943	3502	0.713	0.270	952	3481	0.694	0.305	955	3502	0.785
	17	0.260	958	3481	0.670	0.268	970	3481	0.688	0.270	961	3502	0.695	0.333	984	3523	0.857
	18	0.269	952	3502	0.693	0.280	955	3502	0.720	0.288	935	3481	0.741	0.302	969	3543	0.777
	19	0.264	946	3502	0.678	0.263	972	3481	0.677	0.271	952	3502	0.698	0.321	955	3543	0.826
20	0.266	943	3481	0.683	0.273	969	3481	0.702	0.266	952	3502	0.684	0.338	949	3543	0.869	

Acknowledgements

The experimental facility was developed with the help of the AGH University of Science and Technology in Cracow. The research was supported by the framework of statutory activities, AGH University of Science & Technology, No. 16.16.100.215.

References

Asdrubali F., (2009), A scale model to evaluate water evaporation from indoor swimming pools, *Energy and Buildings*, **41**, 311-319.

ASHRAE Handbook, (2015), ASHRAE Handbook - HVAC Applications, Atlanta, USA, On line at: <https://www.ashrae.org/technical-resources/ashrae-handbook/ashrae-handbook-online>.

Baturin V.V., (1972), *Principles of Industrial Ventilation*, In: *Humidity* 3rd Edition, Pregamon Press, Oxford, UK.

Biasin K., Krumme W., (1974), Evaporation of water in an indoor swimming pool (Die Wasserverdunstung in einem Innenschwimmbad), *Electrowaerme International*, **32**, 115-129.

Blázquez J.L.F., Maestre I.R., Gallero F.J.G., Gómez P.Á., (2017), A new practical CFD-based methodology to calculate the evaporation rate in indoor swimming pools, *Energy and Buildings*, **149**, 133-141.

Bower S.M., Saylor J.R., (2009), A study of the Sherwood-Rayleigh relation for water undergoing natural convection-driven evaporation, *International Journal of Heat and Mass Transfer*, **52**, 3055-3063.

Carrier W.H., (1918), The temperature of evaporation, *ASHRAE Transactions*, **24**, 25-50.

Ciuman P., Lipska B., (2018), Experimental validation of the numerical model of air, heat and moisture flow in an indoor swimming pool, *Building and Environment*, **145**, 1-13.

Hens H., (2009), *Indoor Climate and Building Envelope Performance in Indoor Swimming Pools*, In: *Energy*

Efficiency and New Approaches, Bayazit N., Manioglou G., Oral G., Yilmaz Z. (Eds.), Istanbul Technical University, 543-552.

Himus G.W., Hinchley J.W., (1924), The effect of a current air on the rate of evaporation of water below the boiling point, *Journal of the Society of Chemical Industry*, **43**, 840-845.

Hugo B.R., (2015), *Modeling evaporation from spent nuclear fuel storage pools: A diffusion approach*, PhD Thesis, Washington State University.

Jodat A., Moghiman M., Anbarsooz M., (2012), Experimental comparison of the ability of Dalton based and similarity theory correlations to predict water evaporation rate in different convection regimes, *Heat Mass Transfer*, **48**, 1397-1406.

Kumar N., Arakeri J.H., (2015), Natural convection driven evaporation from a water surface, *Procedia IUTAM*, **15**, 108-115.

Lu T., Lü X., Viljanen M., (2014), Prediction of water evaporation rate for indoor swimming hall using neural networks, *Energy and Buildings*, **81**, 268-280.

Lurie M., Michailoff N., (1936), Evaporation from free water surface, *Industrial and Engineering Chemistry*, **28**, 345-349.

Malicki M., (1962), *Ventilation and Air-Conditioning* (in Polish), PWN Publisher, Warszawa.

Matarazzo A., (2017), Water footprint applied to construction sector, *Environmental Engineering and Management Journal*, **16**, 1739-1749.

Meyer A.F., (1942), *Evaporation from Lakes and Reservoirs: A Study Based on Fifth Years' Weather Bureau Records*, Minnesota Resources Commission, St. Paul, MN, On line at: <http://onlinebooks.library.upenn.edu/webbin/book/lookup?key=ha001485948>.

Pauken M.T., (1999), An experimental investigation of combined turbulent free and forced evaporation, *Experimental Thermal and Fluid Science*, **18**, 334-340.

- Poós T., Varjul E., (2019), Review for prediction of evaporation rate at natural convection, *Heat and Mass Transfer*, **55**, 1651-1660.
- Powell R.W., Griffiths E., (1935), The evaporation of water from plane and cylindrical surfaces, *Transactions Institution of Chemical Engineers*, **13**, 175-198.
- Raimundo M.A., Gaspar R.A., Oliviera A.V., Quintela A.D., (2014), Wind tunnel measurements and numerical simulations of water evaporation in forced convection airflow, *International Journal of Thermal Sciences*, **86**, 28-40.
- Rowher C., (1931), Evaporation from free water surface, Technical Bulletin number 271, US Department of Agriculture, Washington, D.C., USA, On line at: <https://naldc.nal.usda.gov/download/CAT86200265/PDF>.
- Sartori E., (2000), A critical review on equations employed for the calculation of the evaporation rate from free water surfaces, *Solar Energy*, **68**, 77-89.
- Shah M.M., (2003), Prediction of evaporation from occupied indoor swimming pools, *Energy and Buildings*, **35**, 707-713.
- Shah M.M., (2008), Analytical formulas for calculating water evaporation from pools, *ASHRAE Transactions*, **114**, 610-618.
- Shah M.M., (2012), Calculation of evaporation from indoor swimming pools: Further development of formulas, *ASHRAE Transactions*, **118**, 460-466.
- Shah M.M., (2013), New correlation for prediction of evaporation from occupied swimming pools, *ASHRAE Transactions*, **119**, 450-455.
- Shah M.M., (2014), Methods for calculation of evaporation from swimming pools and other water surfaces, *ASHRAE Transactions*, **120**, 3-17.
- Shah M.M., (2018), Improved model for calculation of evaporation from water pools, *Science and Technology for the Built Environment*, **24**, 1064-1074.
- Smith C.C., Löf G., Jones R., (1993), Energy requirements and potential savings for heated indoor swimming pools, *ASHRAE Transactions*, **99**, 429-439.
- Smith C.C., Löf G., Jones R., (1994), Measurement and analysis of evaporation from an inactive outdoor swimming pool, *Solar Energy*, **53**, 3-7.
- Smith C.C., Löf G.O.G., Jones R.W., (1998), Rates of evaporation from swimming pools in active use. *ASHRAE Transactions*, **104**, 514-523.
- Tang R., Etzion Y., (2004), Comparative studies on the water evaporation rate from a free water surface and that from a free surface, *Building and Environment*, **39**, 77-86.
- VDI 2089, (2010), Building services in swimming baths - Indoor pools (Sheet 1. Technical building equipment for swimming pools - indoor pools). VDI Society for Building and Building Technology.